

11-16-1995

Target Geometry Dependence of Electron Energy Loss Spectra in Scanning Transmission Electron Microscopy (STEM)

A. Rivacoba

Universidad del Pais Vasco/Euskal Herriko Unibertsitatea, waprioca@sq.ehu.es

J. Aizpurura

Universidad del Pais Vasco/Euskal Herriko Unibertsitatea

N. Zabala

Universidad del Pais Vasco/Euskal Herriko Unibertsitatea

Follow this and additional works at: <https://digitalcommons.usu.edu/microscopy>



Part of the [Biology Commons](#)

Recommended Citation

Rivacoba, A.; Aizpurura, J.; and Zabala, N. (1995) "Target Geometry Dependence of Electron Energy Loss Spectra in Scanning Transmission Electron Microscopy (STEM)," *Scanning Microscopy*. Vol. 9 : No. 4 , Article 1.

Available at: <https://digitalcommons.usu.edu/microscopy/vol9/iss4/1>

This Article is brought to you for free and open access by the Western Dairy Center at DigitalCommons@USU. It has been accepted for inclusion in Scanning Microscopy by an authorized administrator of DigitalCommons@USU. For more information, please contact digitalcommons@usu.edu.



TARGET GEOMETRY DEPENDENCE OF ELECTRON ENERGY LOSS SPECTRA IN SCANNING TRANSMISSION ELECTRON MICROSCOPY (STEM)

A. Rivacoba*, J. Aizpurua and N. Zabala

Departamento de Física de Materiales, Facultad de Química,
Universidad del País Vasco/Euskal Herriko Unibertsitatea, Apto. 1072, 20080 San Sebastian, Spain

(Received for publication May 6, 1995 and in revised form November 16, 1995)

Abstract

In the frame of the Self-Energy formalism, we study the interaction between STEM electrons and small particles in the range of the valence electron excitations. We first calculate the energy loss probability for an isolated sphere and study the loss spectrum dependence on the size of the particle and on the relative impact parameter. Then we analyze the loss spectra in more realistic situations: (a) the effect of the coupling between the particle and supporting surface is studied in a simple geometrical model; and (b) we analyze the dependence of the losses on the geometrical shape of the target by considering hemispherical particle. Our results are in a good qualitative (and in simple cases, quantitative too) agreement with several experimental results which show anomalous excitations. We restate the suitability of the dielectric theory to study the surface excitations of these systems.

Key Words: Scanning transmission electron microscopy (STEM), electron energy losses, plasmons, small particles, surfaces.

Introduction

In the last decade, electron energy loss spectroscopy (EELS) in scanning transmission electron microscopy (STEM), has been widely used in the study of small catalysts and semiconductor devices. The first small particle EELS experiments were performed by Fujimoto and Komaki (1968), by using a broad beam. The further development of the STEM has allowed one to use a narrow 100 KeV beam of about 0.5 nm width. Under those conditions, Batson (1980; 1982a,b; 1985), Cowley (1982), and Howie (1983) performed the first experiments showing the ability of this technique to reveal structural details of the target. In those experiments, some anomalous energy loss peaks were related to the coupling between the particle and the support. Wang and Cowley (1987a,b,c,d), working with Al particles and different supports, and Ugarte *et al.* (1992), with Si spheres, have reported similar effects. Ouyang *et al.* (1992) studied the size dependence of the surface plasmon energy in Ag particles lying on a carbon surface. They found that the classical dielectric theory does not explain these data, and suggested that for particles larger than 10 nm some quantal effect occurs. Walsh (1989) found results for small Al particles in an AlF₃ matrix, and discussed them in terms of dielectric excitation theory of a two-phase medium. They showed that the experiments cannot be interpreted in terms of any available effective medium theory.

The classical dielectric theory using a bulk local dielectric description of the target, has described in detail the surface excitations in some electron energy loss experiments (Howie and Milne, 1984, 1985; Marks 1982; Schattschneider, 1989). For STEM electrons, non-local corrections are relevant only if the electron travels at very small distances from the interface during most of its flying time (Echenique, 1985; Zabala and Echenique, 1990). The first theoretical approach to the problem of a sphere was made by Fujimoto and Komaki (1968) considering a broad beam and a Drude dielectric function. Schmeits (1981), Kohl (1983), and Ferrell and Echenique (1985) studied the case of a well focused

*Address for correspondence:

Alberto Rivacoba,
Univ. País Vasco, Euskal Herriko Unibertsitatea
Dpto. Física Materiales,
Apto. 1072,
20080 San Sebastian,
Spain

Telephone number: 34 43 216600
FAX number: 34 43 212236
E.mail: waprinoa@sq.ehu.es

Symbol Table

$P(\omega)$	Energy loss probability.
$W(\mathbf{r}, \mathbf{r}', \omega)$	Screened interaction.
$\phi_0(\mathbf{r})$	Microprobe wave packet.
$g(\mathbf{r}-\mathbf{b})$	Transversal profile of the beam.
v	Velocity of the charge.
\mathbf{r}	Position of the charge.
a	Radius of the sphere.
b	Impact parameter.
Z_a	Half the distance the charge travels in the medium.
ω	Energy of an elemental excitation.
ω_l	energy of the l^{th} mode in a sphere.
ω_p	Bulk plasmon energy.
$\epsilon(\omega)$	Dielectric response function.
$\rho(\mathbf{r}, \omega)$	ω -component of the charge density.
$\beta_l(\omega)$	Surface response function.
k_c	Cut-off momentum.
$Y_{lm}(x)$	Spherical harmonic.
$Ci(x)$	Cosine integral function.
$P_{lm}(x)$	Legendre functions.
$K_m(x)$	Modified Bessel function of order m .

beam interacting with a sphere. This problem has been generalized to the cases of coated spheres (Echenique *et al.*, 1987a), penetrating trajectories (Bausells *et al.*, 1987; Echenique *et al.*, 1987b; Rivacoba and Echenique, 1990; Tran Thoai and Zeitler, 1988a,b), and spheroids (Illman *et al.*, 1988). The coupling between two metallic spheres has been worked out by Schmeits and Dambly (1991). Fusch and Barrera (1995), and Martin Moreno and Pendry (1995) have solved the dielectric response of a system of spheres. Rivacoba *et al.* (1995) have studied cylindrical surfaces.

In this paper, we present a procedure to calculate the energy loss probability which is suitable in many situations of interest in STEM. It is useful in the case of EELS from small particles. To illustrate the process of using this method, the problem of the isolated sphere is solved in a general case. Then, we analyse the effects in the loss spectra introduced by the support surface and by the shape of the particle in relation to the isolated sphere case. These results agree with many experimental results.

Theoretical approach

The probability $P(\omega)$ of losing energy ω experienced by a probe interacting with a surface has been calculated

in the frame of a self-energy formalism, where the microprobe is described by means of a quantal wave packet, while the target excitations are given by the local bulk dielectric function of the target (Echenique *et al.*, 1987b). In the case of a very narrow electron beam, travelling along the z -axis at impact parameter b , the energy loss probability is given by the following equation (we use atomic units throughout this paper):

$$P(\omega) = \frac{1}{\pi v^2} \int dz \int dz' \text{Im} \left\{ W(\mathbf{r}, \mathbf{r}', \omega) \exp[-i \frac{\omega}{v} (z-z')] \right\} \quad (1)$$

(Rivacoba *et al.*, 1992) where $W(\mathbf{r}, \mathbf{r}', \omega)$ is the screened interaction; i.e., the solution of the equation $\epsilon(\omega) \nabla^2 W(\mathbf{r}, \mathbf{r}', \omega) = \delta(\mathbf{r}-\mathbf{r}')$ which verifies the boundary condition at the interfaces. This function brings all the information about the response of the target to the external field; i.e., one can easily obtain the potential induced by any external probe in terms of this function. The finding of $W(\mathbf{r}, \mathbf{r}', \omega)$ reduces to an electrostatic like problem which can be solved in a standard way. In eq. (1), the screened interaction is evaluated at the points z and z' of the trajectory; i.e., at the point (b, z) and (b, z') . In this calculation, the recoil of the electron has been neglected. The validity of this approximation for STEM electrons has been stated by Ritchie (1981).

Equation (1) leads to the known formulae for simple target geometries such as planes, films, cylinders or spheres. Although eq. (1) was first obtained by using a quantal description of the probe, it also can be obtained considering the probe as a classical particle (Zabala and Rivacoba, 1993). Eq. (1) provides a general way to deal with coupled or complicated geometries of practical interest in electron microscopy.

This expression is also useful for an extended beam. In a more realistic situation, where the microprobe is more broad, in the direction perpendicular to z -axis, it can be represented by a wave-packet centered at the impact parameter b

$$\Phi_0(\mathbf{r}) = g(\mathbf{r}_\perp - \mathbf{b}) \exp[ik_0 z] \quad (2)$$

where \mathbf{r}_\perp is the projection of \mathbf{r} on the XY plane. Here the function $|g(\mathbf{r}_\perp - \mathbf{b})|^2$ describes the transversal profile of the beam. Ritchie and Howie (1988) have proved that when all the inelastically scattered electrons are collected, the probability of losing energy ω is given by:

$$P(\omega) = \int d\mathbf{r}_\perp |g(\mathbf{r}_\perp - \mathbf{b})|^2 P_{\text{clas}}(\omega, \mathbf{b}) \quad (3)$$

where $P_{\text{clas}}(\omega, \mathbf{b})$ is the energy loss experienced by a classical electron at impact parameter \mathbf{b} . In most of the experimental conditions, the semi-angle of acceptance is large enough ($\vartheta \approx 8 \cdot 10^{-3}$ radians) that the condition of collecting all the scattered electrons is fulfilled. This result is interesting because it states that the interaction

of a broad beam can be considered as the incoherent sum of inelastic processes corresponding to classical particles.

Equation (1) can be better understood if we rewrite it in the following way

$$P(\omega) = \frac{1}{\pi} \int dr \int dr' \text{Im} \left\{ \rho(r',\omega) W(r,r',\omega) \rho^*(r,\omega) \right\} \quad (4)$$

where $r(r,\omega)$ is the ω -component of the charge density corresponding to the incoming charge., and ρ^* stands for its conjugate complex. Equation (4) shows that the energy loss probability $P(\omega)$ is the value of the imaginary part of the screened interaction averaged over the trajectory. This last equation is more general than eq. (1), and can be applied to study problems when the electron trajectories are no longer a straight line, as in the case of reflections from surfaces (Rivacoba, 1994).

Spherical targets

Now we apply the above equations to the case of the interaction of the STEM beam with a spherical target of radius a characterized by the dielectric function $\epsilon_1(\omega)$. In order to consider the most general case, we suppose that the particle is embedded in an infinite medium of dielectric function $\epsilon_2(\omega)$.

To calculate the screened interaction; we expand this function in the appropriate multipolar series in each region of the space. The coefficients of those expansions are obtained by imposing to the function and its normal derivative the standard boundary conditions of continuity at the surfaces; when these conditions are satisfied, and when $r < a$; $r' < a$, we have:

$$W(r,r',\omega) = \frac{1}{\epsilon_1(\omega)} \sum_{l,m=-1}^1 \sum_{r_>} \frac{4\pi}{2l+1} \frac{r_<}{r_>^{l+1}} Y_{lm}^*(\Omega') Y_{lm}(\Omega) + \sum_{l,m=-1}^1 \frac{4\pi}{2l+1} [\beta_l(\omega) - \frac{1}{\epsilon_1(\omega)}] \frac{(r r')^l}{a^{2l+1}} Y_{lm}^*(\Omega') Y_{lm}(\Omega) \quad (5-a)$$

Here $r_<$ and $r_>$ stand for the smallest and largest of both r and r' , and $Y_{lm}(\Omega)$ are the corresponding spherical harmonics.

When both points, r and r' , are outside the sphere ($r > a$; $r' > a$) the screened interaction is given by:

$$W(r,r',\omega) = \frac{1}{\epsilon_2(\omega)} \sum_{l,m=-1}^1 \sum_{r_>} \frac{4\pi}{2l+1} \frac{r_<}{r_>^{l+1}} Y_{lm}^*(\Omega') Y_{lm}(\Omega) + \sum_{l,m=-1}^1 \frac{4\pi}{2l+1} [\beta_l(\omega) - \frac{1}{\epsilon_2(\omega)}] \frac{a^{2l+1}}{(r r')^{l+1}} Y_{lm}^*(\Omega') Y_{lm}(\Omega) \quad (5-b)$$

In both expressions the first series $\{in 1/\epsilon_1(\omega) \text{ or } 1/\epsilon_2(\omega)\}$ corresponds to the direct Coulomb term in a non-bounded medium, while the second ones are the surface induced terms.

Finally, when $r_< < a$ and $r_> > a$, the screened interaction is expressed as:

$$W(r,r',\omega) = \sum_{l,m=-1}^1 \frac{4\pi}{2l+1} \beta_l(\omega) \frac{r_<}{r_>^{l+1}} Y_{lm}^*(\Omega') Y_{lm}(\Omega) \quad (5-c)$$

The surface response function $\beta_l(\omega)$ is given by

$$\beta_l(\omega) = \frac{2l+1}{l\epsilon_1 + (l+1)\epsilon_2} \quad (6)$$

Now we evaluate, by means of eq. (1), the energy loss probability for a STEM electron moving with velocity v parallel to the Z-axis in a trajectory which penetrates the sphere, with impact parameter $b < a$.

Special attention should be paid to the direct Coulombian terms in eqs. (5-a) and (5-b). The contributions of those terms can be written as the quantity corresponding to the energy loss in an infinite medium plus a bulk correction due to the presence of the surface. To illustrate this point, we now consider the contribution T_1 to the total energy loss probability coming from the Coulombian term in eq. (5-a).

$$T_1 = \frac{1}{\pi v^2} \int_{-z_a}^{z_a} dz \int_{-z_a}^{z_a} dz' \text{Im} \left\{ \frac{1}{\epsilon_1(\omega)} \sum_{l,m} (2-\delta_{m0}) \frac{(l-m)!}{(l+m)!} \frac{r_<}{r_>^{l+1}} P_{lm}(\cos \vartheta) P_{lm}(\cos \vartheta') \exp \left[i \frac{\omega}{v} (z-z') \right] \right\} \quad (7)$$

where $r^2 = b^2 + z^2$, P_{lm} are the Legendre functions, the polar angle ϑ is evaluated at the point z of the trajectory i.e.: $\cos \vartheta = z/r$, and $z_a = (a^2 - b^2)^{1/2}$ is half the length of the trajectory inside the sphere. Then we rewrite this term as follows:

$$T_1 = \frac{1}{\pi v^2} \int_{-z_a}^{z_a} dz \int_{-\infty}^{\infty} dz' \text{Im} \left\{ \frac{1}{\epsilon_1(\omega)} \sum_{l,m \geq 0} (2-\delta_{m0}) \frac{(l-m)!}{(l+m)!} \frac{r_<}{r_>^{l+1}} P_{lm}(\cos \vartheta) P_{lm}(\cos \vartheta') \exp \left[i \frac{\omega}{v} (z-z') \right] \right\} - \frac{1}{\pi v^2} \int_{-z_a}^{z_a} dz \left[\int_{-\infty}^{-z_a} dz' + \int_{z_a}^{\infty} dz' \right] \text{Im} \left\{ \frac{1}{\epsilon_1(\omega)} \sum_{l,m \geq 0} (2-\delta_{m0}) \frac{(l-m)!}{(l+m)!} \frac{r_<}{r_>^{l+1}} P_{lm}(\cos \vartheta) P_{lm}(\cos \vartheta') \exp \left[i \frac{\omega}{v} (z-z') \right] \right\} \quad (8)$$

The first term corresponds to the energy loss experienced by an electron travelling a distance $2z_a$ through a non-bounded medium of dielectric function ϵ_1 . Note that the screened interaction in this term is merely the Coulomb potential, i.e., $[(1/\epsilon_1) \{1/(b^2 + (z-z')^2)^{1/2}\}]$; in this way, it is easy to prove that the contribution of this term is proportional to the distance $2z_a$. The use of a local dielectric response function leads to divergent values for this bulk term. This divergence can be removed by considering the momentum dependence of the dielectric function, which cancels the large momentum transfer contribution to the induced potential.

The second term in eq. (8) is finite and provides a correction to the bulk excitation probability due to the fact that the polarizable medium is no longer infinite. Using the Cartesian expression of the screened interaction, it is simple to prove that T_1 can be written as follows:

$$T_1 = \frac{4z_a}{\pi v^2} \text{Im} \frac{-1}{\epsilon_1(\omega)} \ln \left\{ \frac{vk_c}{\omega} \right\} + \frac{2}{\pi v^2} \text{Im} \frac{-1}{\epsilon_1(\omega)} \int_0^{2z_a} dz \text{Ci} \left[\frac{z\omega}{v} \right] \quad (9)$$

where the first term is the bulk probability in an infinite medium comes from the first term of eq. (8). Here a cut-off momentum k_c has been used to avoid the large momentum transfer contribution. The second term is the bulk correction appearing in eq. (8). Here, $\text{Ci}(x)$ is the cosine integral function. This last term remains always finite, even though $\text{Ci}(x)$ diverges logarithmically for small arguments (Abramowitz and Stegun, 1965).

In the same way, one could handle the other Coulombian term in eq. (5-b). After some algebra, one obtains the total energy loss probability. The surface contribution (without the direct bulk terms) is then given by:

$$P(\omega; a, b) = \frac{-4a}{\pi v^2} \sum_l \sum_{m \geq 0} (2 - \delta_{m0}) \frac{(l-m)!}{(l+m)!} \left\{ \text{Im} \left\{ \frac{2l+1}{l\epsilon_1 + (l+1)\epsilon_2} \right\} [A_{lm}^0 + A_{lm}^i]^2 - \text{Im} \frac{1}{\epsilon_1(\omega)} [(A_{lm}^0)^2 + A_{lm}^i A_{lm}^0]^2 - \text{Im} \frac{1}{\epsilon_2(\omega)} [(A_{lm}^i)^2 + A_{lm}^i A_{lm}^0]^2 \right\} \quad (10)$$

the ω dependent functions A_{lm}^i and A_{lm}^0 are given by the following equations:

$$A_{lm}^i = \int_0^{z_a} dz \frac{r^l}{a^{l+1}} P_{lm} \left(\frac{z}{r} \right) g_{lm} \left(\frac{z\omega}{v} \right)$$

$$A_{lm}^0 = \int_{z_a}^{\infty} dz \frac{r^l}{r^{l+1}} P_{lm} \left(\frac{z}{r} \right) g_{lm} \left(\frac{z\omega}{v} \right) \quad (11)$$

here the function $g_{lm}(x)$ is $\sin(x)$ when $(l+m)$ is odd or $\cos(x)$ otherwise. This equation was first found in the frame of the classical theory (Rivacoba and Echenique, 1990).

The surface contribution to the total excitation probability given by eq. (10) is twofold: the first term containing the surface response function $\beta_1(\omega)$ provides the (positive) probability of exciting the surface plasmons, while the second and third terms represent a negative correction to the bulk probability of both dielectric media. This correction is to be added to the direct terms (proportional to the path length) which have been omitted in eq. (10). This is the so-called Bregenzung effect, first predicted by Ritchie (1957) in films. It has been found in other surfaces (Boersch *et al.*, 1968; Rivacoba *et al.*, 1994; Schmeits 1981).

In the case of a metallic sphere in vacuum, the energy of the surface modes are given by the equation $l\epsilon + (l+1) = 0$; which leads to the well-known plasmon frequencies:

$$\omega_l = \sqrt{\frac{l}{2l+1}} \omega_p \quad l=1,2,\dots \quad (12)$$

An interesting analytical property of the Bregenzung effect is that it verifies that the sum of the probabilities of exciting surface modes has the same functional form, but opposite sign, as the sum of the bulk correction in both media. It explains the fact that when the probe travels through an interface, the surface excitations occur at expense of the number of bulk plasmons excited in both media. Formally this fact can be expressed

$$\sum_l P(\omega_l) = - [\Delta P_{\text{bulk } 1}(\omega_{p1} \rightarrow \omega_l) + \Delta P_{\text{bulk } 2}(\omega_{p2} \rightarrow \omega_l)] \quad (13)$$

where $\Delta P_{\text{bulk } 1,2}$ is the bulk correction of the medium 1 or 2.

In the case of non-penetrating trajectories ($b > a$) $A_{lm}^i = 0$, while the A_{lm}^0 has been analytically evaluated by using the following relation (Ferrell *et al.*, 1987):

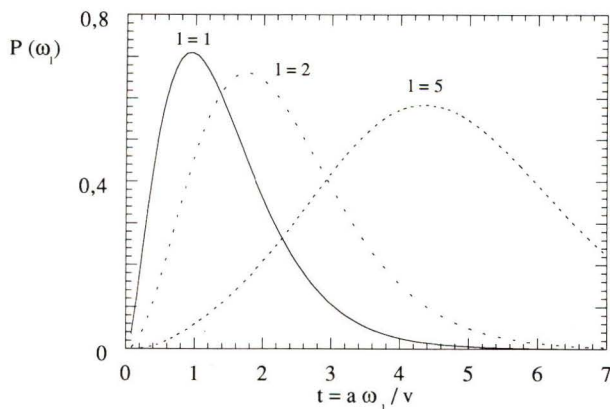


Figure 1. Contribution of the first l -th multipolar terms to the total loss probability as a function of the radius, in a metallic sphere. A Drude dielectric function has been considered.

$$\int_{-\infty}^{\infty} \frac{dz}{\sqrt{b^2+z^2}} P_{lm}\left(\frac{z}{\sqrt{b^2+z^2}}\right) \exp(ikx) = 2 \left[\frac{ik}{|k|}\right]^{l-m} \frac{|k|^l}{(l-m)!} K_m(lkb) \quad (14)$$

where K_m are the modified Bessel functions. The surface contribution to the energy loss probability is then given by the following equation:

$$P(\omega; a,b) = \frac{4a}{\pi v^2} \sum_l \sum_{m \geq 0} \frac{(2-\delta_{m0})}{(l-m)!(l+m)!} \text{Im} \left\{ \frac{2l+1}{\epsilon_1 + (l+1)\epsilon_2} - \frac{1}{\epsilon_2(\omega)} \right\} \left[\frac{\omega a}{v}\right]^{2l} K_m^2\left(\frac{\omega b}{v}\right) \quad (15)$$

first obtained by Ferrell and Echenique (1985). These authors pointed out the fact that many multipolar terms are needed in order to compute eq. (15) accurately. To illustrate this point, in Figure 1, we plot the contribution of different multipolar terms to $P(\omega; a,b)$ as a function of the radius of the particle for a metallic target. The dipolar and quadrupolar terms are only relevant for spheres of radius about $v\omega^{-1}$; for larger particles higher multipolar excitations are the most relevant contribution to the spectrum. The energy of these modes is given by eq. (12) and tends very fast to the planar plasmon energy $\omega_s = \omega_p (2)^{-1/2}$. Therefore, for large spheres ($a \gg v\omega^{-1}$), the spectrum presents, in this case, a single peak around ω_s ; similar to that corresponding to a planar surface. Echenique *et al.* (1987a) have analytically proven that the planar approach to this problem, i.e., to

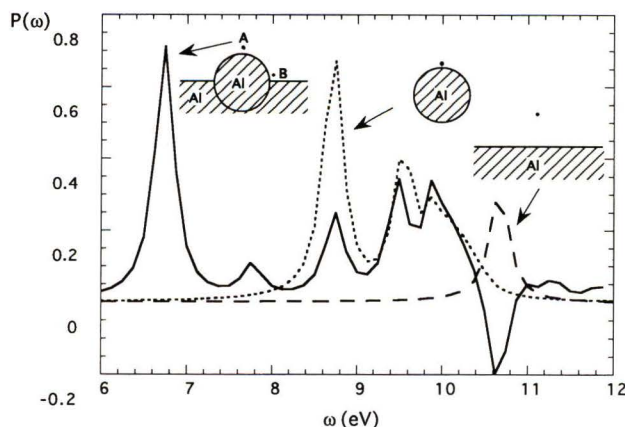


Figure 2. Spectra corresponding to an Al sphere half embedded in Al (continuous line). The sphere radius is 10 nm and the impact parameter $b = 11$ nm. The beam position is marked as A in the scheme. The dotted line corresponds to an isolated sphere under the same conditions, and the dashed line corresponds to a planar Al surface of length $2a$. Beam energy is 100 keV.

consider the sphere as a planar surface at any point of the trajectory with an instantaneous impact parameter, leads to the same equation as eq. (15) in the limit of large values of a .

Particle Coupled to a Planar Surface

In most of the experimental conditions, the target is lying on a large supporting substrate, therefore the former development is just a first approach to the real problem. The former approach seems reasonable in the case of metallic particles on an insulating supporting surface but it is not suitable to some problems where the particle and the support are of the same medium. Several authors (Batson, 1982a,b; Wang and Cowley, 1987a,b,c,d; Ugarte *et al.*, 1992) have reported some anomalous effects on supported spherical particles, which are probably due to the coupling between both surfaces.

One simple geometrical model to deal with this problem is that of a sphere of radius a and dielectric functions $\epsilon_1(\omega)$, half-embedded in a semi-infinite medium of dielectric functions $\epsilon_2(\omega)$ limited by a planar surface as shown in the upper scheme of Figure 2.

In the case of electron trajectories parallel to the planar surface, the energy loss probability can be obtained in the same way as shown in the previous section. Following Zaremba (1985), the particle contribution to screened interaction is written as a multipolar expansion, while the contribution corresponding to the direct Coulomb and planar image potential are directly added. The coefficients of this expansion are calculated by imposing

the matching conditions on the interfaces. This procedure leads to a set of linear algebraic equations where all the coefficients of the multipolar series are coupled. Then the problem of finding the screened interaction can no longer be analytically calculated and numerical procedures are required. To do so, the expansion has to be truncated. In general, even for small spheres, many multipolar terms are needed to get good stability of the solution. Working with the computed multipolar series, one calculates the contribution of the particle to the energy loss spectrum through eq. (1). The total spectrum would consist of the particle contribution plus the contribution of the planar interface. This last contribution is proportional to the path length (Echenique and Pendry, 1975), and therefore in our geometric model, where the planar interface is infinite, is infinite too. Nevertheless, this geometric model is reasonably suitable for situations where the real length of the supporting surface is much larger than $v\omega^{-1}$.

First we study the dependence of energy loss spectrum on the beam position. We have calculated the energy loss probability $P(\omega)$ in the case of an Al sphere lying on an Al surface. In this case, a Drude dielectric function with small damping has been used ($\omega_p = 15.1$ eV, $\gamma = 0.27$ eV). The beam energy is 100 keV. Out of simplicity, only non-penetrating trajectories have been considered. In Figure 2, we show the particle contribution to the loss spectrum calculated when the electron beam travels near the top of the particle. By comparing this spectrum to that of an isolated sphere, we realize that the main effect of the supporting surface is the presence of a new, very narrow and tall resonance at 6.8 eV which compensates the lowering of the 8.7 eV dipolar peak in the spectrum corresponding to the isolated sphere. The position of the 6.8 peak does not depend either on the size of the sphere or on the relative beam/target position; thus, this resonance is a new interface mode associated with the coupling particle/support. This peak presents a monopolar charge distribution, and can be explained as due to the grounding of the particle by the metallic support. Above 9.5 eV, the spectrum is rather similar to that corresponding to an isolated sphere. It has been proven that this latter peak presents a radius dependence similar to that shown in Figure 1. The absolute intensity of this excitation falls down very fast for values larger than $v\omega^{-1}$. For larger particles, the support effect is negligible (at this particular beam position).

The spectrum of Figure 2 presents a negative peak in the neighborhood of 10.7 eV. This peak is due to the fact that we plot the particle contribution to the total energy loss, then the planar surface contribution should be added. This last spectrum (dashed line) consists of a peak centered at the planar surface plasmon, just

where the negative values occur. This is a sort of compensation effect: negative values of $P(\omega)$ in this region means that there is a lowering of the total probability of exciting planar surface plasmon, which is compensated by the excitations of surface modes corresponding to the particle. This negative surface peak can be explained by noting that one of the effects of the sphere is to reduce the effective length of the planar surface, responsible of the energy losses at this region.

The former 6.8 eV peak practically disappears when the beam travels near the edge (at the position marked B in Figure 2). The most relevant part of this spectrum consists of some broad resonance above the planar surface plasmon energy ω_s .

To study the influence of the dielectric nature of the support, we now consider an Al particle at a AlF_3 surface which at this energy range is an insulator. Experimental data have been used for both media {Hagemman HJ, Gudat W, Kunz C (1974) unpublished Desy report SR74/7; Walsh, 1989}. The spectrum shown in Figure 3 corresponds to the beam position marked as A. Note that, as in the former case, the dipolar peak of the isolated sphere has almost disappeared, and a new small peak at 7.3 eV has taken its place. The remaining part of the spectrum is broader but it does not differ significantly from that corresponding to the isolated particle.

Experimental observation on metallic particles are in qualitative agreement with these results. Batson (1982a,b) has compared the experimental spectra in the case of a small (10 nm) Al particle when the support is a larger Al sphere to that corresponding to an insulator support. The only difference between the spectra was the presence of a peak at 4 eV in the case of the metallic support which did not appear in the case of the insulator support. The remaining part of the surface excitation spectra was almost identical and basically consisted of one surface peak centered at 7 eV. The 4 eV resonance did not appear in the case of Al support when the beam position was at the edge formed by the plane and the sphere. The differences between the experimental and theoretical values of the low energy peak are probably due to two facts: (a) the target geometry is not the same; and (b) in the experimental situation, the particles have an oxide layer, which is clearly visualized in the 23 eV filtered images. The effect of the oxide coating is to shift down the loss peak.

Hemispherical Particles

Ouyang *et al.* (1992) have reported very accurate experimental data about the size dependence of the surface loss peak energy of STEM electrons interacting with Ag hemispheres lying on C surface. The high

Target geometry dependence of EELS in STEM

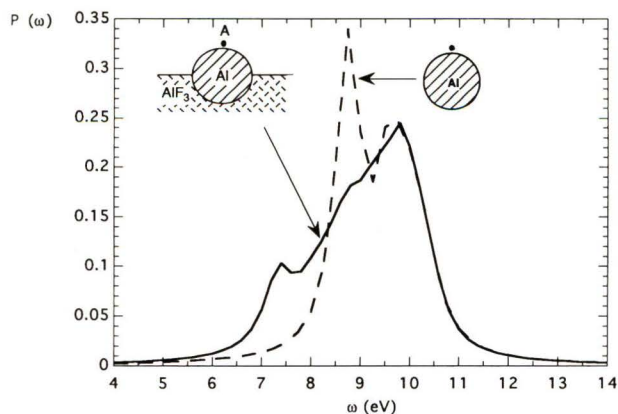


Figure 3. Spectra corresponding to an Al sphere half embedded in Al F₃ (continuous line) for the same position as in Figure 2. The dashed line corresponds to an isolated sphere in vacuum. Beam energy is 100 keV.

resolution of these data (about 0.1 eV), and the fact that the silver surface is free of oxide layers, allow a test of the suitability of the classical dielectric theory to describe the surface excitations in this energy region. Those authors found that the energy of the peak shifts down with the size in the region of (2-8 nm) getting a minimum value $\omega = 3.1$ eV for particles of about 10 nm; and then the peak energy grows to reach the 3.5 eV. The authors compare these results to that of a development of the classical dielectric theory and conclude that these results cannot be explained by this theory. The shift of the plasma frequency in small particles has been theoretically studied (Apell and Ljungbert, 1982), and a recent work on Ag particles (Tiggesbäumker *et al.*, 1993) agrees with the data reported by Ouyang *et al.* (1992). We focus our interest on particles larger than 10 nm (in diameter) where one should expect the classical dielectric theory to provide a good description of the target excitations.

Using the same approach as in the previous sections, we have studied this problem by considering a hemispherical target. We proceed in the same way as in the previous section: computing the screened interaction and then calculating the energy loss probability. Technically, the problem is quite similar, and its details are to be reported elsewhere. Because of the finite size of the target, eq. (1) allows study of any electron trajectory; nevertheless, we are going to consider only non-penetrating trajectories parallel to the planar surface of the particle.

To illustrate the surface excitations of this geometry, we show, in Figure 4, the spectra corresponding to an Al hemispherical particle, for two positions of the beam. When the beam travels near the top of the particle (position A), the spectrum does not differ very much from that corresponding to an isolated sphere under similar

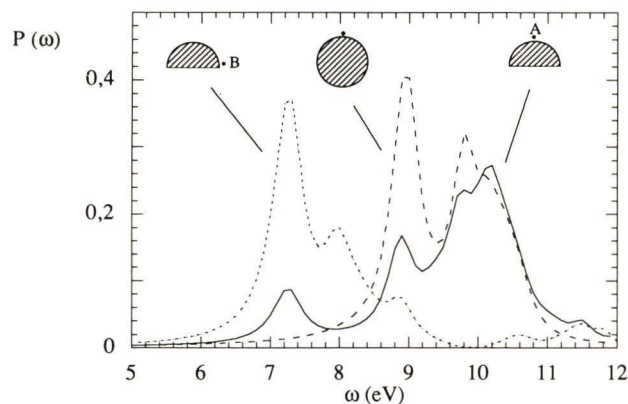


Figure 4. Spectra corresponding to an Al hemisphere of radius 10 nm. Solid and dotted lines correspond to beam positions marked as A and B, respectively. The spectrum corresponding to an isolated sphere (dashed line) is shown. The particle travels 1 nm from the surface in all the cases.

conditions; the new spectrum presents a lowering in the peaks which correspond to dipolar and quadrupolar excitations of the isolated sphere, and a small new peak appears at 7.1 eV. The remaining part of the spectrum, corresponding to high multipolar excitations in case of the isolated sphere, remains almost unchanged. On the other hand, when the beam travels near the edge of the particle (position B), the spectrum consists of a main peak around 7.1 eV. Therefore, this resonance is characteristic of the edge of our target. The 7.1 eV peak corresponds to several normal modes of this geometry with very close values of the energy around $0.5 \omega_p$. The charge density of these modes are distributed near the corner formed by the hemisphere and the planar basis of the particle. This fact explains why the probability of this excitation becomes maximum for beam position close to the edge, while in the case of the beam at the top position, the electron notices a quasi-spherical surface, and, in comparison to the sphere, only the low multipolar modes are disturbed and the change introduced by the missing hemisphere in the high multipolar modes are not so relevant in this case. In this position, the influence of the corner, i.e., of this particular target geometry, is small, and in consequence, the 7.1 eV peak is small. When the beam position moves to the corner, this last contribution becomes the most relevant. In Figure 4, spectra corresponding to the two extreme positions of the beam are shown; for intermediate positions, both peaks are present in the spectrum.

The former results depend on the size of the particle. At position A, the smaller the particle is, the larger the corner contribution becomes. For large hemispheres, this geometry does not differ from that of a

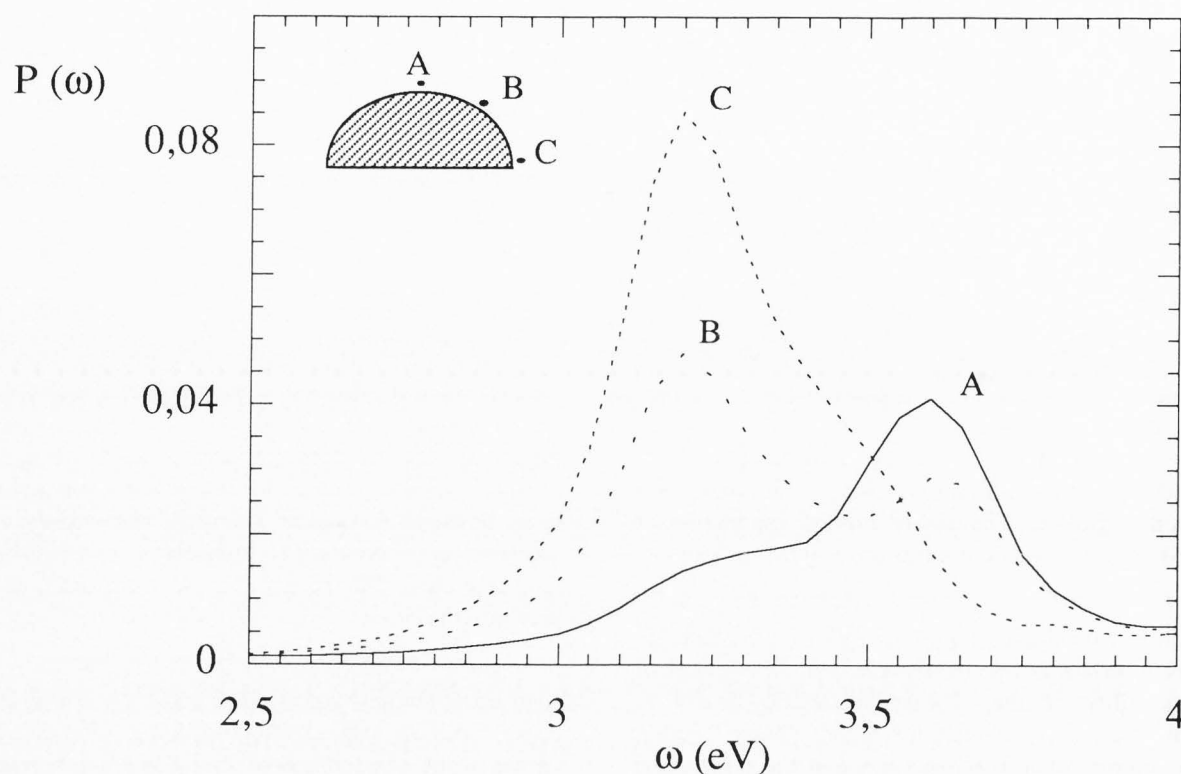


Figure 5. Spectra corresponding to a silver hemisphere of radius 5 nm, for three positions of the beam. The particle travels 1 nm from the surface in all the cases.

plane; then, the spectrum should consist of a peak at the surface plasmon energy and the 7.1 eV peak is negligible.

Now we apply the former results to the case of Ag hemispheres. Experimental values of the Ag dielectric function have been used (Palik, 1985). In Figures 5 and 6, the spectra corresponding to two hemispheres of different sizes are shown for three different beam positions. As in the Al case, the contribution of the two resonances are clear, but in the case of the small particle, the low energy excitation at 3.2 eV is, at almost any beam position, more relevant than the higher mode at 3.6 eV. A spectrum obtained by averaging over the beam position would present a peak, centered at about 3.2 eV. For the largest particle, we see that the most relevant contribution is that at 3.6 eV, and the averaged spectrum should have its peak near this value. For particle size in-between, the relative intensity of both modes will be similar, and one could expect the averaged spectrum being centered at intermediate values.

This size dependence of the energy of the loss peak agrees pretty well with the experimental data reported by Ouyang *et al.* (1992). The shift of 0.1 eV in the energy between both theoretical and experimental results is

probably due to the coupling of the hemisphere to the carbon substrate. A rough evaluation of the carbon support effect has been published (Rivacoba *et al.*, 1994) and proves that this effect shifts the peak energy down by a few tenths of an eV. Note that the use of other dielectric data for the Ag (Hagemman *et al.*, 1974, unpublished report) can move the overall spectrum downwards by a few tenths of an eV.

The fact that Ouyang and Isaacson (1989) cannot explain these results through a classical theory is probably due to some weakness in the theoretical approach they use.

In **conclusion**, we have studied the energy loss spectra of STEM electrons interacting with a small particle, and their dependence on the shape of the target, and on the impact parameter. The dipolar peak is not significant in many experimental situations due to the effect of the support, or to the non-spherical shape of the particle. Some anomalous energy peaks found in pre-existing experimental results are explained, as due to these effects. The impact dependence of these anomalous peaks can provide information about the target. Finally, we state the suitability of the dielectric theory to these problems as it was for planar interfaces.

Target geometry dependence of EELS in STEM

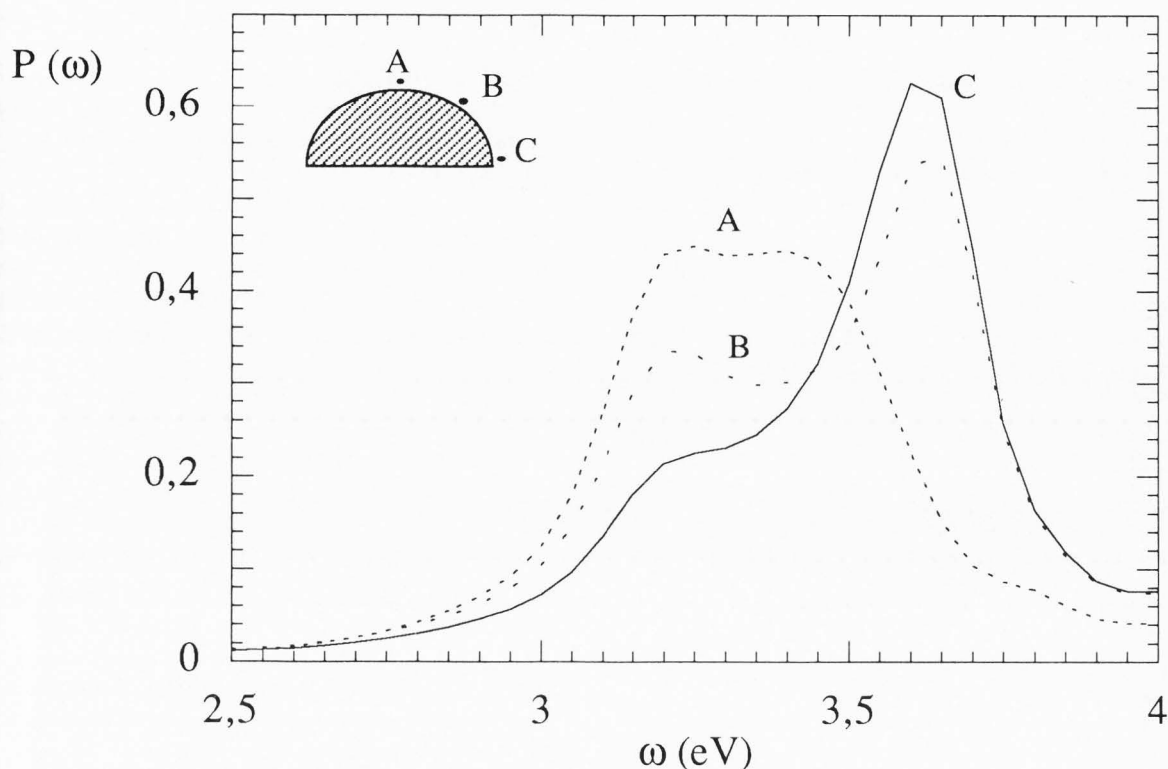


Figure 6. Spectra corresponding to a silver hemisphere of radius 40 nm, for three positions of the beam. The particle travels 1 nm from the surface in all the cases.

Acknowledgements

The authors gratefully acknowledge Prof. Ritchie and Prof. Echenique for many stimulating discussions. They also thank Gipuzkoako Foru Aldundia and the Basque Country Government (Eusko Jaurlaritz) for financial help.

References

- Abramowitz M, Stegun IA (1965) Handbook of Mathematical Functions. Dover, New York. pp. 231-233.
- Apell P, Ljungbert Å (1982) Red shift of surface plasmons in small metal particles. *Solid State Comm.* **44**, 1367-1369
- Batson PE (1980) Damping of bulk plasmons in small aluminum spheres. *Solid State Comm.* **34**, 477-480.
- Batson PE (1982a) Surface plasmon coupling in clusters of small spheres. *Phys. Rev. Lett.* **49**, 936-940.
- Batson PE (1982b) New surface plasmon resonance in clusters of small Al spheres. *Ultramicroscopy* **9**, 277-282.
- Batson PE (1985) Inelastic scattering of fast electrons in clusters of small spheres. *Surf. Sci.* **156**, 720-784.
- Bausells J, Rivacoba A, Echenique PM (1987) Energy loss in spheres by penetrating electrons. *Surf. Sci.* **189/190**, 1015-1022.
- Boersch H, Geiger J, Stickel W (1968) Anregung von Kristallgitterschwingungen durch Elektronenstrahlen. *Z. Phys.* **212**, 130-145.
- Cowley JM (1982) Surface energies and structure of small crystals. *Surf. Sci.* **114**, 587-606.
- Echenique PM (1985) Dispersion effects in the excitation of interfaces by fast-electron beams. *Phil. Mag.* **B52**, L9-L13.
- Echenique PM, Pendry JB (1975) Absorption profile at surfaces. *J. Phys.* **C8**, 2938-2942.
- Echenique PM, Howie A, Wheatley DJ (1987a) Excitation of dielectric spheres by external electron beams. *Phil. Mag.* **B56**, 335-349.
- Echenique PM, Bausells J, Rivacoba A (1987) Energy-loss probability in electron microscopy. *Phys. Rev.* **B35**, 1521-1524.
- Ferrell TL, Echenique PM (1985) Generation of surface excitations on dielectric spheres by an external electron beam. *Phys. Rev. Lett.* **55**, 1526-1529.
- Ferrell TL, Warmack RJ, Anderson VE, Echenique

- PM (1987) Analytical calculation of stopping power for isolated small spheres. *Phys. Rev.* **B35**, 7365-7371.
- Fujimoto AA, Komaki K (1968) Plasma oscillations excited by a fast electron in a metallic particle. *J. Phys. Soc. Jpn.* **25**, 1679-1687.
- Fusch R, Barrera RG (1995) Theory of the energy loss in a random system of spheres. *Phys. Rev.* **B52**, 3256-3273.
- Howie A (1983) Surface reactions and excitations. *Ultramicroscopy* **11**, 141-148.
- Howie A, Milne RH (1984) Electron energy loss spectra and reflection images from surfaces. *J. Microsc.* **136**, 279-285.
- Howie A, Milne RH (1985) Excitations at interfaces and small particles. *Ultramicroscopy* **18**, 427-434.
- Illman BL, Anderson VE, Warmack RJ, Ferrell TL (1988) Spectrum of surface-mode contributions to the differential energy-loss probability for electrons passing by a spheroid. *Phys. Rev.* **B38**, 3045-3049.
- Kohl H (1983) Image formation by inelastically scattered electrons: Image of a surface plasmon. *Ultramicroscopy* **11**, 53-65.
- Marks LD (1982) Observation of the image force for fast electrons near an MgO surface. *Solid State Comm.* **43**, 727-729.
- Martin Moreno L, Pendry JB (1995) Electron energy loss in dense arrays of metallic particles. *Nucl. Instrum. Methods Phys. Res.* **B96**, 565-568.
- Ouyang F, Isaacson M (1989) Accurate modeling of particle-substrate coupling of surface plasmon excitation in EELS. *Ultramicroscopy* **31**, 345-350.
- Ouyang F, Batson PE, Isaacson M (1992) Quantum size effects in the surface-plasmon excitation of small metallic particles by electron-energy-loss-spectroscopy. *Phys. Rev.* **B46**, 15421-15425.
- Palik ED (ed.) (1985) *Handbook of Optical Constants of Solids*. Academic Press, London. pp. 350-359 and 394-403.
- Ritchie RH (1957) Plasma losses by fast electrons in thin films. *Phys. Rev.* **106**, 874-881.
- Ritchie RH (1981) Quantal aspects of the spatial resolution of the energy-loss measurements in electron microscopy. *Phil. Mag.* **A44**, 931-942.
- Ritchie RH, Howie H (1988) Inelastic scattering probabilities in scanning transmission electron microscopy. *Phil. Mag.* **A59**, 753-767.
- Rivacoba A (1994) Surface corrections to bulk energy losses in STEM. *Proc. 15th Werner Brandt Workshop.* **99**, 195-199 (copy available from A. Rivacoba).
- Rivacoba A, Echenique PM (1990) Surface correction to bulk energy losses in scanning transmission electron microscopy of spheres. *Scanning Microsc.* **4**, 73-78.
- Rivacoba A, Zabala N, Echenique PM (1992) Theory of energy loss in scanning transmission electron microscopy of supported small particles. *Phys. Rev. Lett.* **69**, 3362-3365.
- Rivacoba A, Zabala N, Apell P (1994) Energy loss of STEM electrons in coupled surfaces. *Surf. Sci.* **307-309**, 867-873.
- Rivacoba A, Apell P, Zabala N (1995) Energy loss probability of STEM electrons in cylindrical surfaces. *Nucl. Instrum. Methods Phys. Res.* **B96**, 465-469.
- Schattschneider P (1989) The dielectric description of inelastic electron scattering. *Ultramicroscopy* **28**, 1-15.
- Schmeits M (1981) Inelastic scattering of fast electrons by spherical surfaces. *J. Phys.* **C14**, 1203-1216.
- Schmeits M, Dambly L (1991) Fast-electron scattering by bispherical surface-plasmon modes. *Phys. Rev.* **B44**, 12706-12712.
- Tiggesbäumker J, Köller L, Meiwes-Broer K, Liebsch A (1993) Blue shift of the Mie plasma frequency in Ag clusters and particles. *Phys. Rev.* **A48**, 1749-1752.
- Tran Thoai DB, Zeitler E (1988a) Multipole surface excitations on small oxide-covered metal particles by fast electrons. *Appl. Phys.* **A45**, 249-253.
- Tran Thoai DB, Zeitler E (1988b) Inelastic scattering of fast electrons by small metal particles. *phys. stat. sol.* **A107**, 791-797.
- Ugarte D, Colliex C, Trebbia P (1992) Surface- and interface- plasmon modes on small semiconducting spheres. *Phys. Rev.* **B45**, 4332-4343.
- Walsh C (1989) Analysis of electron energy-loss spectra from electron-beam-damaged amorphous AlF₃. *Phil. Mag.* **A59**, 227-246.
- Wang ZL, Cowley JM (1987a) Surface plasmon excitation for supported metal particles. *Ultramicroscopy* **21**, 77-94.
- Wang ZL, Cowley JM (1987b) Size and shape dependence of the surface plasmon frequencies for supported metal particle systems. *Ultramicroscopy* **23**, 97-108.
- Wang ZL, Cowley JM (1987c) Excitation of the supported metal particle surface plasmon with external electron beam. *Ultramicroscopy* **21**, 335-346.
- Wang ZL, Cowley JM (1987d) Generation of surface plasmons excitation of supported metal particles by an external electron beam. *Ultramicroscopy* **21**, 347-366.
- Zabala N, Echenique PM (1990) Energy loss of fast electrons moving near plane boundaries with dispersive media. *Ultramicroscopy* **32**, 327-335.
- Zabala N, Rivacoba A (1993) Electron energy loss near supported particles. *Phys. Rev.* **B48**, 14534-14542.
- Zaremba E (1985) Van der Waals interaction between an atom and a surface defect. *Surf. Sci.* **151**, 91-102.

Discussion with Reviewers

M. Schmeits: Is it possible, within the used method, to obtain, for the studied geometries, the values of the surface plasmon frequencies (either analytically or numerically) and the distribution of the corresponding charge oscillations?

Authors: Yes, it can be done. Note that the induced potential $\phi(\mathbf{r}, \omega)$ can be written in terms of our screened interaction, $W(\mathbf{r}, \mathbf{r}', \omega)$ as follows:

$$\phi(\mathbf{r}, \omega) = \int d\mathbf{r}' W(\mathbf{r}, \mathbf{r}', \omega) \rho(\mathbf{r}, \omega)$$

where $\rho(\mathbf{r}, \omega)$ is the ω -component of the charge density. Therefore, the plasmons frequencies correspond to the values of ω for which a non-trivial solution of Laplace equations exists. In the cases studied here, as in other problems involving coupled surfaces, as for instance, in your Schmeits and Dambly (1991) paper, this procedure leads to a coupling between all the multipolar terms, for each value of the azimuthal number m , which has to be solved numerically. In the same way, it is possible to get the charge density on the interface.

We are writing an extended paper about these problems.

M. Schmeits: In particular, what is the charge (or potential) distribution and symmetry of the surface plasmon responsible for the lowest peak of the loss function of the hemispherical geometry for electron trajectories passing close to the corner?

Authors: There are several modes contributing to this peak. The energies of these modes are very close to $0.5 \omega_p$. One simple description of charge density of the lowest mode ($m = 1$) consists of piling the charge of different sign up in the opposite corners of the hemisphere.

P.E. Batson: You imply with Figure 1, that if a is about v/ω , then modes having small angular momentum dominate the response. But, in the case of aluminium, where v/ω is about 150 \AA for the surface loss, the planar surface plasmon energy is obtained for b near to a , even for particles in the $50\text{-}100 \text{ \AA}$ range. It seems to me that the more important condition, which by itself can force the response to small angular momentum modes, is that b must be much bigger than a . Please comment.

Authors: Figure 1 corresponds to an isolated metallic sphere, an idealized situation which is not reachable under experimental conditions. In this case, for grazing incidence ($b \cong a$), it is easy to prove analytically, from eq. (15), that the maximum of the probability of exciting the l^{th} multipolar mode occurs when $a \cong 1 (v/\omega_l)$ as illustrated in Figure 1. You are correct in pointing out

that at large impact parameters, the dipolar peak dominates the loss spectra; this can be understood from the same eq. (15) by taking into account the exponential asymptotic behaviour of the Bessel functions.

In our opinion, the fact that in experiments with small $\{(a\omega_l/v) < 1\}$ Al particles, the loss peak appears at frequencies close to the surface plasmon energy is due to the coupling between the particle and other surfaces. In the spectra shown in Figures 2, 3 and 4, the dipolar peak has been shifted down or almost removed, in comparison to the isolated particle spectra; then, the main feature of these spectra is a peak around the surface plasmon energy. In the case of supported particles, the shifted low energy peak is present too in the experiments {see, for instance, your own Batson (1985) paper}.

P.E. Batson: In your Figures 2 and 3, there appear to be two mechanisms whereby peaks are shifted or created: (1) In Figure 3, the $l = 1$ surface mode is shifted downwards by the presence of the AlF_3 dielectric; and (2) in Figure 2, the $l = 1$ surface mode of the isolated sphere is replaced by a surface mode having lower symmetry characterized by the sphere/plane system, and caused by anti-symmetric coupling of normal modes which are characteristic of the sphere and the plane separately. Is this an accurate view?

Authors: This could be an intuitive and simple description of the effects of the coupling between both interfaces. Although, in this problem, all the multipolar terms are involved in this new mode, the more relevant mode is the dipolar one, and therefore, your explanation is basically correct.

P. Schattschneider: Can you comment on conditions under which coherence effects would be important, contrary to eq. (3)? If that would be the case for smaller collection angles, could there be consequences, e.g., a search for these coherence effects, using nanoprobe in the TEM?

Authors: The limits to the suitability of eq. (3) are placed by the existence of electrons scattered with a momentum transfer large enough as not to be collected by the experimental set up in the acceptance angle. The probability of such excitations does not depend on the target size, unless the target is large enough as to make multiple scattering processes possible.

P. Schattschneider: Ugarte *et al.* (1992) and Walsh (1989) measured plasmon spectra in small Si spheres and in microholes, respectively. Both groups found qualitative agreement with electrodynamics calculations. Is your theoretical approach able to explain the as yet unexplained details in any of these experiments?

Authors: The results reported by Ugarte *et al.* (1992)

have been studied as an application of the problem of the half embedded particle in the paper (Zabala and Rivacoba, 1993); in this work, the loss peak is shifted downwards 1 or 2 eV. For a better quantitative agreement with the experiment, one should consider the problem of two small slightly interpenetrating spheres. Arguably the modes of such a system take place at lower energy.

The results by Walsh (1989), seem to be a problem of an effective medium since there are many coupled Al particles in an AlF_3 matrix.